BBA Advances 7 (2025) 100140

Contents lists available at ScienceDirect

BBA Advances

journal homepage: www.sciencedirect.com/journal/bba-advances

Extracellular vesicles display distinct glycosignatures in high-grade serous ovarian carcinoma

Kristina Mae Bienes [a], Akira Yokoi [b,c,**], Masami Kitagawa [b], Hiroaki Kajiyama [b], Morten-Thaysen Andersen [a,d], Rebeca Kawahara [a,*]

[a] Institute for Glyco-core Research (iGCORE), Nagoya University, Emergent/Innovative Engineering Building Room 815, Furo-cho, Chikusa-ku, Nagoya, Aichi 464-8601, Japan
[b] Department of Obstetrics and Gynecology, Nagoya University Graduate School of Medicine, 65 Tsurumai-cho, Showa-ku, Nagoya 466-8550, Japan
[c] Nagoya University Institute for Advanced Research, Japan
[d] School of Natural Sciences, Macquarie University, Australia

ARTICLE INFO

Keywords:
N-glycans
Glycoproteins
Extracellular vesicles
High grade serous carcinoma
Biomarker
Glycoproteomics
Ascites
Ovarian cancer

ABSTRACT

High-grade serous ovarian carcinoma (HGSOC) is a deadly subtype of ovarian cancer (OC), often diagnosed at late stages due to nonspecific symptoms and lack of effective markers for early detection. Aberrant protein N-linked glycosylation has been reported in HGSOC, holding a potential for improving the diagnosis and prognosis of affected patients. Building on our recent observation documenting that HGSOC-derived extracellular vesicles (EVs) exhibit aberrant protein expression patterns, we here explore the protein N-glycosylation displayed by EVs isolated from HGSOC cell lines and patient ascites relative to those from matching controls to unveil candidate markers for HGSOC. Comparative glycoproteomics of small EVs (sEVs, <200 nm) and medium/large EVs (m/lEVs, >200 nm) isolated from HGSOC and non-cancerous cell lines revealed lower overall N-glycosylation of EV proteins and a decreased protein expression of oligosaccharyltransferase (OST) subunits from HGSOC compared to non-cancerous cell lines. Increased α2,6-sialylation was also observed in m/lEVs from HGSOC cell lines and patient ascites by lectin blotting, which correlated with increased gene expression of *ST6GAL1* and decreased gene expression of *ST3GAL3/4* in HGSOC compared to normal ovary tissues. Our study provides insights into the EV glycoproteome of HGSOC and the underlying changes in the glycosylation machinery in HGSOC tissues, opening new avenues for the discovery of novel markers against HGSOC.

Abbreviations

AAL	aleuria aurantia lectin
ACN	acetonitrile
ConA	concanavalin A
cryo-EM	cryo-electron microscopy
DTT	dithiothreitol
EVs	extracellular vesicles
FA	formic acid
FDR	false discovery rate
GEPIA	gene expression profiling interactive analysis
glycoPSMs	glycopeptide-to-spectral matches
GTEx	genotype-tissue expression
HCD	higher-energy collision-induced dissociation
HGSOC	high-grade serous ovarian carcinoma
IgG	immunoglobulin G
LC-MS/MS	liquid chromatography-tandem mass spectrometry
MALII	Maackia amurensis lectin II
mRNA	messenger ribonucleic acid
MS	mass spectrometry
NeuAc	N-acetylneuraminic ccid
NTA	nanoparticle tracking assay
OC	ovarian cancer
OST	oligosaccharyltransferase
PBS	phosphate buffered saline
PCA	principal component analysis
PVDF	polyvinylidene fluoride
sEVs	small extracellular vesicles

* Corresponding author.
** Co-corresponding author.
E-mail addresses: ayokoi@med.nagoya-u.ac.jp (A. Yokoi), rebeca.kawahara@igcore.nagoya-u.ac.jp (R. Kawahara).

https://doi.org/10.1016/j.bbadva.2025.100140
Received 22 October 2024; Received in revised form 6 January 2025; Accepted 9 January 2025
Available online 10 January 2025
2667-1603/© 2025 The Authors. Published by Elsevier B.V. This is an open access article under the CC BY-NC-ND license (http://creativecommons.org/licenses/by-nc-nd/4.0/).

m/lEVs medium/large extracellular vesicles
non-glycoPSMs non-glycosylated peptide-to-spectral matches
SNA sambucus nigra agglutinin
ST6GAL1 β-galactoside α-2,6-sialyltransferase 1
ST3GAL3/4 β-galactoside α-2,3-sialyltransferase 3/4
TFA trifluoroacetic acid
TCGA the cancer genome atlas.

Introduction

Ovarian cancer (OC) is the 8th most common cancer and the 5th leading cause of cancer-related deaths in women [1]. Despite advances in medical research, OC remains a significant public health concern due to its often late-stage diagnosis and complex treatment challenges. Early diagnosis is particularly challenging for high-grade serous ovarian carcinoma (HGSOC), a deadly and most common subtype of OC [2]. More than 60% of HGSOC cases in OC patients are identified only after the cancer has metastasized to other organs [2]. The survival rate for HGSOC diagnosed at early stages (I, II) is approximately 90%, whereas only 20–40% of patients with advanced stages (III, IV) survive beyond five years post-diagnosis [3]. Current early-stage OC biomarkers lack specificity and sensitivity, highlighting the need for further biomarker research for this disease.

Extracellular vesicles (EVs) are membrane-enclosed particles that bud from cells. In cancer, EVs transport cancer-derived molecules that are critical mediators of cell communication facilitating cancer progression and spread [4]. Because cancer-derived EVs are released into biological fluids such as serum, ascites and urine, they hold a potential to carry biomarkers for the HGSOC detection and monitoring of treatment responses [5]. However, EVs are heterogeneous in size and content posing a major challenge in the identification of HGSOC-specific markers [6].

Aiming to finding new markers for HGSOC detection, we recently profiled the proteome of two distinct EV populations: small EVs (sEVs, <200 nm) and medium/large EVs (m/lEVs, > 200 nm) shed from HGSOC-like cancerous and non-cancerous cell lines and patient serum and ascites [7]. While several HGSOC membrane marker candidates (e.g. FRα and TACSTD2) were reported, their post-translational modifications including glycosylation, which is known to impact their function, were not addressed in that study. Aberrant glycosylation has indeed been repeatedly reported in OC, leading to significant interest in exploring the glycobiology related to OC and utilizing these abnormal glycosylation patterns for diagnosing and predicting the progression of the disease [8–10]. Nevertheless, the glycoproteome of OC-derived EVs and their potential for early detection of OC remains unexplored.

Herein, we interrogated new and previously published proteomics data to explore the N-glycoproteome signatures of sEVs and m/lEVs isolated from cell lines and patient sera and ascites in HGSOC and used tissue transcriptomics data to investigate the underlying changes in the glycosylation machinery in HGSOC cell lines and tissues. Glycoproteomics revealed less efficient (under-glycosylation) of HGSOC-derived EV proteins, an observation that was accompanied by reduced levels of OST subunits in HGSOC compared to non-cancer cells. Elevated α2,6-sialylation was observed in HGSOC-derived m/lEVs from both cell lines as well as patient ascites, which correlated with increased *ST6GAL1* and decreased *ST3GAL3/4* gene expression in HGSOC relative to normal tissues. This study details the aberrant glycosylation displayed by HGSOC-specific EVs opening new biomarker opportunities to improve the diagnosis and survival of HGSOC patients.

Materials and methods

Published data origin

This study reinterrogated previously published proteomics LC-MS/MS raw data from sEVs, m/lEVs and cell lysate fractions originating from six ovarian cancer cell lines, KURAMOCHI, COV362, CAOV3, OVCAR3, OV90, and SKOV3 lines and four noncancer cell lines, including HOSE1, HOSE2, HFF2T, and MTK [7]. Proteomics data obtained from ovary tissues and sEVs and m/lEVs isolated from stage III to IV HGSOC patient serum and ascites were also re-interrogated for the identification of glycopeptides [7]. The details of the tissue collection and isolation of EVs from cell lines and patient samples are described in the methods from our previous study [7].

Collection of ascites

Written informed consent was obtained from all patients. Three ascites samples of patients aged 48, 55 and 69 years old, with stage III to IV HGSOC were collected during surgery at Nagoya University Hospital, Nagoya, Japan between 2022 and 2023. Three ascites collected from control patients with benign gynecological tumors aged 49, 56, and 67 years old were collected at Nagoya University Hospital. Ascites samples were centrifuged at 300 *g* undiluted for 5 min at 4 °C to remove cell debris and stored at −80 °C until further use. This study was conducted with the approval by the Institutional Review Board of Nagoya University Hospital (no. 2017–0053).

EV isolation from ascites

sEVs and m/lEVs were isolated from ascites samples from HGSOC patient (n = 3) and benign control patients (n = 3) using ultracentrifugation, following the minimal information for studies of extracellular vesicles (MISEV2023) guidelines [11]. Briefly, approximately 1 ml ascites was centrifuged at 10,000 g for 40 min at 4 °C in the Kubota Model 7000 ultracentrifuge. The pellet was washed in PBS and centrifuged again under the same conditions to suspend the pellet and extract m/lEVs. The m/lEV pellets were resuspended in PBS. The supernatant was filtered using a 0.45 μm filter (Millex-HV 13 mm, Millipore). Albumin and IgG were removed using the ProteoExtract Albumin/IgG Removal Kit (Merck & Co. Inc., USA) and samples were then ultracentrifuged at 110,000 g for 90 min at 4 °C using an MLS50 rotor (Beckman Coulter Inc., USA). The pellet was washed with PBS, ultracentrifuged with the same conditions, and resuspended in PBS to extract sEVs. Protein concentration of EVs was determined using a Qubit protein assay kit (Thermo Fisher Scientific) with the Qubit 4.0 Fluorometer (Invitrogen Co., MA, USA), according to the manufacturers' protocol.

Nanoparticle tracking assay

The size distribution and particle concentration in the EV preparations were analyzed using a NanoSight NS300 (Malvern Panalytical Ltd., UK) nanoparticle tracking analyzer. Samples were diluted in PBS, injected into the measuring chamber, and EV flow was recorded in triplicate measurements (30 s each) at room temperature. Equipment settings for data acquisition were kept constant between measurements, with camera level set to 13.

Cryo-electron microscopy (EM)

The isolated EVs were visualized using a cryo-EM (Terabase Inc., Okazaki, Japan) that can generate high-contrast images of the nanostructures of biological materials without staining procedures that may damage the samples. The natural structure of the sample distributed in solution can be observed by preparing the sample using a rapid vitreous ice-embedding method.

Proteomics analysis of ascites

Lysis of the isolated EV populations was performed using 4 M urea. Protein extracts (10 μg) were reduced using 10 mM DTT (30 min, 30 °C) and alkylated using 40 mM iodoacetamide (final concentrations, 30 min,

in the dark, 20 °C). Alkylation reactions were quenched using excess DTT. Proteins were digested using sequencing grade porcine trypsin (1:50, w/w; 12 h, 37 °C, Promega). Proteolysis was stopped by acidification using 1% (v/v) trifluoroacetic acid (TFA, final concentration). Peptides were desalted using primed Oligo R3 reversed phase solid phase extraction (SPE) micro-columns as described [12] and dried.

Peptides were loaded on a PepMap™ Neo Nano Trap Cartridge (5 mm × 300 μm inner diameter, Thermo) and separated on an analytical column (Aurora Ultimate; 25 cm × 75 μm, 1.7 μm ID, IonOpticks) at 300 nl/min provided by an Vanquish Neo UHPLC System (Thermo). The mobile phases were 99.9% ACN in 0.1% (both v/v) FA (solvent B) and 0.1% (v/v) FA (solvent A). The gradient was 3–35% B over 90 min, 35–50% B over 8 min, 50–90% B over 2 min, and 10 min at 95% B. The nanoLC was connected to an Orbitrap Exploris 240 mass spectrometer (Thermo) operating in positive ion polarity mode. The Orbitrap was used to acquire full MS1 scans (m/z 380–1800, AGC: Standard, 100 ms maximum accumulation, 120,000 FWHM resolution at m/z 200). Employing data-dependent acquisition within 3s cycle time, the most abundant precursor ions from each MS full scan were isolated and fragmented utilizing higher-energy collision-induced dissociation (HCD, NCE 30%). Only multicharged precursors ($Z \geq 2$) were selected for fragmentation. Fragment spectra were acquired in the Orbitrap (15,000 resolution, AGC: Standard, maximum injection time mode "auto", m/z 1.4 precursor isolation window, 20 s dynamic exclusion after a single isolation/fragmentation of a given precursor).

Glycopeptide profiling

HCD-MS/MS data from previous [7] and newly acquired proteomics data were searched for intact glycopeptides with Byonic (v5.2, Protein Metrics) using 10/20 ppm as the precursor/product ion mass tolerance, respectively. Cys carbamidomethylation (+57.021 Da) was considered fixed modifications. Fully tryptic peptides were searched with up to two missed cleavages per peptide. The following variable modifications were selected allowing two common and one rare modification per peptide: Met oxidation (+15.994 Da, common) and N-glycosylation of sequon-localized Asn (rare) employing a predefined glycan database of 309 mammalian *N*-glycans available within Byonic from which NeuGc compositions were manually removed and HexNAc1, HexNAc1Fuc1, HexNAc2 and HexNAc2Hex3Fuc1 added. The HCD-MS/MS data were searched against all human proteins (20,518 sequences, UniProtKB, released March 2024). All searches were filtered to <1% false discovery rate (FDR) at the glycoprotein level and 0% FDR at the glycopeptide level using a protein decoy database. Only confident glycopeptide identifications (PEP 2D < 0.001) were considered.

Proteomics data analysis

For protein identification and quantification, the raw files were imported into MaxQuant v2.5.2.0. The Andromeda search engine was used to search the HCD-MS/MS data against the reviewed UniProtKB Human Protein Database (released March 2024; 20,418 entries) with a precursor and product ion mass tolerance of 4.5 ppm and 20 ppm, respectively. Carbamidomethylation of cysteine (57.021 Da) was set as a fixed modification. Oxidation of methionine (15.994 Da) and protein N-terminal acetylation (42.010 Da) were selected as variable modifications. All identifications were filtered to < 1% FDR at the protein and peptide level using a conventional decoy approach. For label-free AUC-based quantification, the 'match between runs' feature of MaxQuant was enabled with a 0.7 min match time window and 20 min alignment time window. Protein abundance was calculated based on the normalized protein intensity (LFQ intensity).

Lectin blotting of cell lines and ascites samples

Protein extracts (total 1 μg) were diluted in 15 μl loading buffer containing 1 x Laemmli buffer (BioRad) and 50 mM DTT. The samples were boiled at 95 °C for 5 min. Proteins were separated on a 5–20% SuperSep™ Ace SDS-PAGE gel (FujiFilm) at 100 V and 30 mA for 1 h Afterwards, the gels were transferred onto a PVDF membrane (BioRad) using the Trans-blot SD semi-dry transfer cell (BioRad) at 10 V for 1 h The transferred membrane was blocked with 10 ml Carbo-Free blocking buffer (1:10 dilution, Vector Laboratories) and incubated for 1 h on a shaker. The membrane was incubated with 10 ml Concanavalin A (ConA), *Aleuria Aurantia* Lectin (AAL), *Sambucus Nigra* Agglutinin (SNA) or *Maackia Amurensis* Lectin II (MAL II) (1:2000 dilution, all from Vector Laboratories) in Carbo-Free blocking buffer at 4 °C overnight. The following day, the membrane was washed with 0.1% (v/v) TBS-Tween for 10 min, three times, with shaking. After washing, the membrane was incubated with Streptavidin-HRP (1:1500 dilution, Vector Laboratories) diluted in a Carbo-Free blocking buffer and 0.01% (v/v) TBS-Tween for 1 h The membrane was washed with 0.1% (v/v) TBS-Tween for 10 min, three times, with shaking. The membrane was incubated with 500 μl Immobilon Western HRP substrate (Millipore) for less than 1 min to achieve chemiluminescence. The membrane was imaged using the Amersham ImageQuant 800 (Cytiva). Densitometry analysis was performed using Amersham ImageQuant 800 software (Cytiva).

Gene expression profile

Gene expression (mRNA) data of ovarian serous cystadenocarcinoma tissues and matched adjacent normal tissues were retrieved from the Cancer Genome Atlas (TCGA) and the Genotype-Tissue Expression (GTEx) portal and interrogated in the Gene Expression Profiling Interactive Analysis (GEPIA) platform. Significance cutoff was set to log2 fold change < 1 and adjusted $p < 0.001$. Data was displayed by boxplots generated in the GEPIA platform [13].

Bioinformatics and statistical analysis

Glycoprotein annotation was performed using Uniprot ID mapping searching for the presence of "glycosylation" term. Glycoproteins detected in at least one of the cell lines in each of the fractions (sEVs, m/lEVs and cell) were considered for further analysis.

Pathway enrichment analysis was performed using DAVID Bioinformatics [14] (National Institute of Health) with corrected $p < 0.05$ as significance threshold. Significance was assessed by unpaired two-tailed Student's T-tests with significant threshold set to 0.05 (95% confidence interval). GraphPad Prism (v9.4.1, Dotmatics) or Perseus v2.0.7.0 were used for statistical analysis. Principal component analysis (PCA) and correlation analysis were performed using MetaboAnalyst v6.0 [15].

Results and discussion

EVs from HGSOC and normal cell lines exhibit distinct N-glycosylation signatures

High-resolution proteomics data of sEVs, m/lEVS and cell lysates fractions isolated from 10 cell lines, including six HGSOC-like ovarian cancer (OV) cells (OVCAR3, KURAMOCHI, OV90, CAOV3, COV362, and SKOV3) and four non-cancerous cell lines (HOSE1, HOSE2, HFF2, and MTK) were re-interrogated for glycoprotein expression patterns and N-glycopeptide signatures missed in the original study [7] (Fig. 1**a**). Owing to the high data quality, a total of 687, 590 and 497 glycoproteins were quantitatively profiled from the LC-MS/MS data across the sEV, m/lEV and cell lysate fractions, respectively (Fig. 1**b** and **Supplementary Tables S1-S2**). The glycoproteins covered 27%, 20% and 12% of the total proteome of sEVs, m/lEVs and cell fractions, respectively, indicating that glycosylation is abundant and enriched in EVs compared to the corresponding cellular fractions. Supporting this finding, a significant increase was observed in the proportion of glycoproteins in sEVs (n

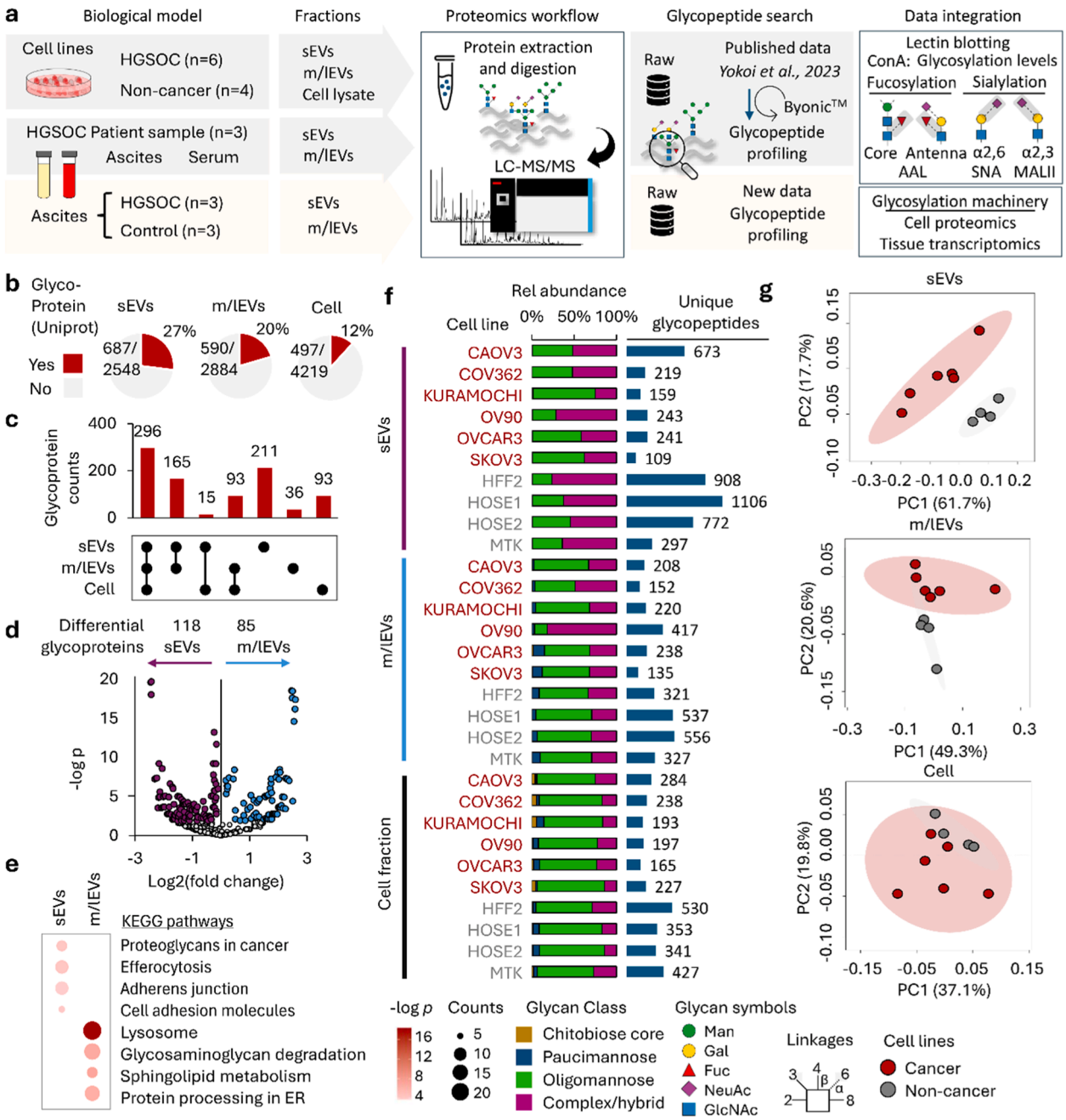

Fig. 1. Glycoproteome profile of sEVs and m/lEVs from HGSOC and normal cell lines. (a) Overview of the experimental approach used to profile glycopeptides from published proteomics data of sEVs and m/lEVs isolated from cell culture supernatant and HGSOC patient ascites and sera [7] and new data of HGSOC and control ascites. (**b**) Proportion of proteins annotated as having the potential to carry glycosylation by UniProt out of all proteins identified in the published proteomics dataset from sEVs, m/lEVs and cell fraction isolated from cell lines. (**c**) Overlap of glycoproteins identified across EVs and cell lysate fractions. (**d**) Differential expression of glycoproteins identified in sEVs vs m/lEVs (n = 10, unpaired T-test, adjusted $p < 0.05$). (**e**) Top 5 most significant KEGG pathways enriched in sEVs and m/lEVs differential glycoproteome. (**f**) Distribution of *N*-glycan classes and number of unique glycopeptides identified across 6 cancerous (red) and 4 non-cancerous ('normal') cell lines (grey) in the sEVs, m/lEVs and cell lysate fractions. (**g**) Glycoprofile comparison between HGSOC and non-cancerous cell lines across the sEV, m/lEV and cell lysate fractions using principal component analysis (PCA).

= 10) and m/lEVs (n = 10) compared to the corresponding cell fractions (n = 10) as determined by the increased glycoprotein ratio in sEVs (2.80 ± 0.49) and m/lEV (1.75 ± 0.35) relative to the cell fractions (**Supplementary Fig. S1a-b**). sEVs displayed the highest number of glycoproteins with 211 glycoproteins uniquely identified in this fraction, in comparison with 38 glycoproteins uniquely identified in m/lEVs. In contrast, a total of 389 glycoproteins were shared between m/lEVs and cell fractions, covering 78.3% of the cell glycoproteome (389/497), indicating high similarity of m/lEVs with the cell glycoproteome (Fig. 1**c**).

Amongst the 816 glycoproteins identified and quantified across the sEV and m/lEV proteome datasets, 203 glycoproteins quantitatively differed between the two EV populations (Fig. 1**d**). A total of 118 glycoproteins were more abundant in sEVs and these were enriched for being involved with cancer and cell adhesion-related pathways (e.g. PTRPF, SCD1, IGF1R), whereas 85 glycoproteins were more abundant in m/lEVs and associated with lysosome and degradation pathways (e.g. HEXA, MAN2B1, CTSC) (Fig. 1**e**). Transmembrane domains, indicating

higher levels of cell surface or intracellular membrane proteins, were found in 84.7% of the differential glycoproteome in sEVs as opposed as 9.4% in m/lEVs (**Supplementary Table S1**).

Re-interrogation of proteomics data identified a total of more than 4800 N-glycopeptides (unique protein, site and glycan) covering more than 1200 glycoproteins across the sEV, m/lEV and cell fractions from the 10 cell lines, missed in the original study [7] (Fig. 1**f, Supplementary Fig. 2a** and **Supplementary Table S3**). Notably, distinct glycosignatures were observed across the different EV populations and between the HGSOC and normal cell systems. While proteins from sEVs were predominantly decorated by complex-type sialylated and fucosylated glycans, the m/lEV proteins were enriched in oligomannosidic- and paucimannosidic-type glycans (**Supplementary Fig. 2b**).

Different mechanisms of EVs biogenesis and cargo selection can drive the differences in the glycoprotein repertoire and glycosylation profile observed between the two EV populations. The biosynthesis of sEVs occurs through the inward budding of endosomal compartments, resulting in the formation of multivesicular bodies that release vesicles upon fusion with the plasma membrane [17]. This process has been linked to the recycling and secretion of many cancer-associated cell surface proteins, which were observed to be significantly over-represented in sEVs (e.g. ADAM17, EPHA2, EPCR, IGF1R) [18,19]. In contrast, m/lEVs are generated by direct outward budding from the plasma membrane, requiring a complex redistribution of phospholipids in the cell surface and coordination of the actomyosin contractile machinery [6]. m/lEVs contain a broad array of molecular cargo, including intracellular trafficking proteins, growth factors and enzymes [20]. Unsupervised clustering showed that m/lEVs and intracellular fractions display similar protein content and glycosylation features (**Supplementary Fig. 3**). Although context and cell type-dependent, complex sialoglycans have been previously reported to be a feature of cell surface glycoproteins, while oligomannosidic glycans are enriched intracellularly [21]. Interestingly, sEVs and m/lEVs displayed similar glycoprofiles from cell surface and intracellular compartments, respectively, highlighting the different cellular content and glycosylation patterns in these two EVs populations. Noteworthy, the less studied truncated glycans spanning chitobiose core ($GlcNAc_2Fuc_{0–1}$) and paucimannosidic ($Man_{1–3}GlcNAc_2Fuc_{0–1}$) glycans [22,23], were found almost exclusively in m/lEVs decorating lysosomal proteins (e.g. SAP, LAMP1, CATD) (**Supplementary Table S3).** Supporting these findings, lysosomal proteins, including the glycoside hydrolases HEXA and HEXB, recently reported to drive the paucimannose biosynthesis [24] were a strong signature in m/lEV (**Supplementary Table S1**). Although lysosomal exocytosis is known to traffic lysosomal proteins to the plasma membrane [25] and extracellular milieu [26,27], the mechanisms driving the selection of lysosomal proteins to m/lEVs are yet to be elucidated.

Next, we aimed to investigate whether the glycoprofile of sEV and m/lEV differs in HGSOC and non-cancerous cell lines. We performed principal component analysis (PCA) of the glycoproteome data collected across different fractions and cell lines. The N-glycoproteome data of sEVs was able to separate HGSOC and non-cancerous cell lines (Fig. 1**g**). In contrast, only partial separation was observed using the N-glycoproteome data of m/lEVs and no separation was achieved using the N-glycoproteome data from the cell lysate fractions. Collectively, these data show that HGSOC-derived EVs carry unique glycosylation signatures.

Glycosylation features of sEVs and m/lEVs from HGSOC and non-cancerous cell lines

Next, we explored the aberrant N-glycosylation features displayed by HGSOC-derived EVs and the underlying mechanisms driving the glycosylation changes. By mapping the total glycopeptide-to-spectral matches (glycoPSMs) relatively to the non-glycosylated peptide-to-spectral matches (non-glycoPSMs), we observed a significant decrease in the overall glycosylation in HGSOC compared to non-cancerous derived EVs, across both the sEV and m/lEV fractions and in the cell lysate fraction (Fig. 2**a**). Using ConA, a lectin with broad glycoepitope recognition (thus a proxy for global glycosylation levels), we further recapitulated the lower glycosylation levels in EVs derived from cancerous compared to non-cancerous cell origins (Fig. 2**b**). To investigate the mechanisms driving the overall lower glycosylation levels in cancerous EVs, we used proteomics data from the cell lysate fraction to map the protein expression of the subunits forming the OST enzyme complex (STT3A/B, RPN1/2, DDOST, DAD1) responsible for N-glycan initiation (**Supplementary Table S2**). Interestingly, lower expression was observed across all the identified OST subunits in HGSOC compared to non-cancerous cell lines, consistent with the overall lower glycosylation efficiency (under-glycosylation) observed in HGSOC-derived EVs (Fig. 2**c**).

OST is sensitive to the cell physiology and reported to be altered in cancer cells [28]. Supporting our findings, Hu et al., reported decreased protein levels of RPN1, RPN2, STT3A and DAD1 in HSGOC compared to normal tissues [29]. Previous reports showed that removal of glycans from the surface of EVs using PNGase F and neuraminidase were associated with increased uptake by recipient cells [30], including ovarian cancer cells [31]. Further studies are needed to investigate the functional consequences of the under-glycosylation of proteins in HGSOC-derived EVs.

Notably, the m/lEVs displayed higher levels of sialic acid containing N-glycopeptides from HGSOC compared to non-cancerous cell lines (Fig. 2**d**). Lectin blotting targeting α2,6- (SNA) and α2,3-sialylation (MALII) showed a shift towards increased levels of α2,6-sialylation in HGSOC-derived m/lEVs (average α2,6/α2,3-linked sialic acid ratio was 1.09 in HGSOC and 0.69 in non-cancerous cell lines, i.e. 1.57-fold higher in HGSOC compared to non-cancerous m/lEVs) (Fig. 2**e and f**). This finding suggests that increased sialylation of N-linked glycans might be primarily driven by increase in α2,6-sialylation.

HGSOC-derived sEVs displayed significantly lower levels of N-glycopeptides carrying single fucose, which represented more than 88% of all fucose-containing glycoPSMs (Fig. 2**g and Supplementary Table S3**). Conversely, AAL lectin staining, which targets both α1,6- and α1,3-fucosyl glycoepitopes showed distinct band patterns across samples albeit similar total intensity levels suggesting similar total levels of fucosylation (Fig. 2**h-i**).

Glycoprofile of EVs isolated from ascites and sera of HGSOC patients

To demonstrate the translational potential of glycofeature detection in EVs from patient samples, we also re-interrogated proteomics data of ovary tissues and sEVs and m/lEVs isolated from ascites and sera collected from HSGOC patients for glycopeptides [7] (**Supplementary Fig. 4a**). Encouragingly, high levels of glycosylation were consistently found in the investigated samples, covering more than 1880 unique N-glycopeptides from 289 proteins (**Supplementary Table S4**). The glycoprofiles of the serum- and ascites-derived EVs correlated between patients, suggesting a common origin of these two EV populations (**Supplementary Fig. 2b**). Recapitulating the findings from the cell lines, the sEVs and m/lEVs clustered separately based on the glycoproteome data, reflecting the different composition and biogenesis of these two fractions (**Supplementary Fig. 4b** and Fig. 1**f**).

We compared the overlap of glycoproteins detected in the sEV and m/lEV populations that are present both in serum, ascites and the originating ovary tissues (**Supplementary Fig. 4c**). A total of 37 and 48 glycoproteins were found in sEVs (e.g. LPR1, VWF, LGALS3BP) and m/lEVs (e.g. SERPINA3, LUM, FETUA), respectively, overlapping across serum and ascites as well as ovary tissues. These commonly expressed glycoproteins represent candidates to be explored in future studies as potential OC-specific biomarkers produced by cancer cells and found both in ascites and serum EVs.

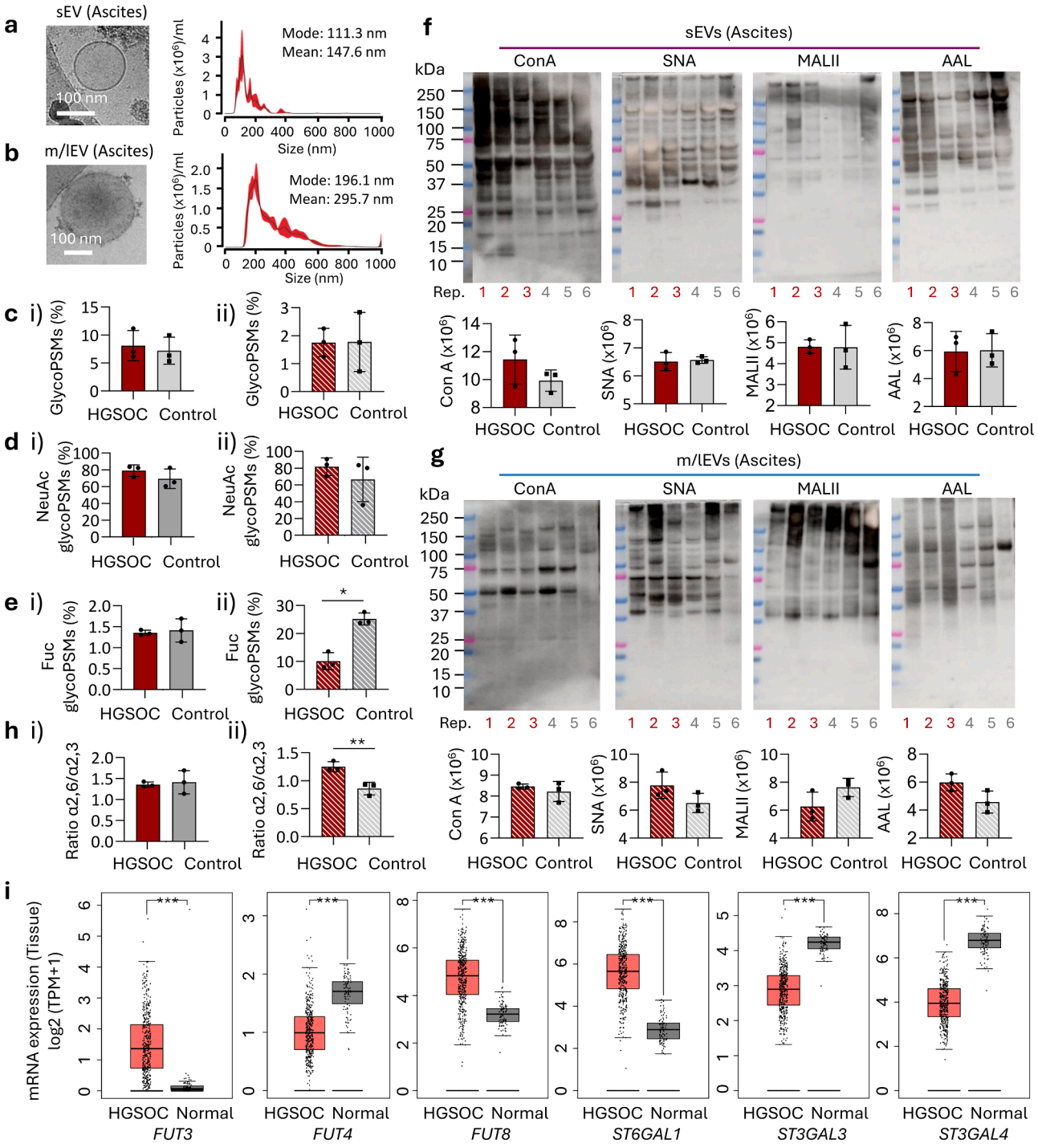

Fig. 2. Aberrant N-glycosylation features in HGSOC-derived EVs. (**a**) Global glycosylation levels of sEV and m/lEV populations as well as cell lysate fractions from HGSOC (n = 6) and non-cancerous (n = 4) cell lines as estimated by the proportion of glycoPSMs relatively to non-glycoPSMs (T-test, *p < 0.05, *** p < 0.001). (**b**) Glycosylation levels assessed using ConA lectin blotting in the sEV, m/lEV and cell lysate fractions from HGSOC (n = 2) and non-cancerous (n = 2) cell lines. (**c**) OST subunit levels based on proteomics data from the cell lysate fractions. (FC = fold change, T-test, cancer, n = 6, non-cancer, n = 4, *p < 0.05). (**d**) Global sialylation levels determined by NeuAc-containing N-glycopeptides relative to total glycoPSMs identified in the sEV, m/lEV and cell lysate fractions isolated from HGSOC (n = 6) and non-cancerous (n = 4) cell lines (T-test, *p < 0.05). Lectin blotting targeting (**e**) α2,6-sialyl epitopes using SNA and (**f**) α2,3-sialyl epitopes using MAL-II in sEV, m/lEV and cell lysate fractions isolated from HGSOC (n = 2) and non-cancerous (n = 2) cell lines. (**g**) Global core fucosylation level as estimated by the presence of mono-fucosylated N-glycopeptides relative to total glycoPSMs in sEV, m/lEV and cell lysate fractions isolated from HGSOC (n = 6) and non-cancerous (n = 4) cell lines (T-test, *p < 0.05). (**h**) α1,6- and α1,3-fucosyl epitopes stained using AAL lectin blotting in the sEV, m/lEV and cell lysate fractions isolated from HGSOC (n = 2) and non-cancerous (n = 2) cell lines. (**i**) Protein loading control by silver staining (1 μg protein).

α2,6-sialylation is elevated in HGSOC-derived m/lEVs from patient ascites

Aiming to explore if the glycosylation features observed in EVs from HGSOC cell lines could be recapitulated in patient-derived EVs, populations of sEVs and m/lEVs were isolated from ascites of HGSOC patients (n = 3) and control patients with benign tumors who underwent surgery (n = 3). Nanoparticle tracking assays (NTAs) and cryo–electron microscopic analyses confirmed the expected size of the isolated sEVs (~100 nm) and m/lEVs (>200 nm) from ascites (Fig. 3**a-b**). Proteomics data revealed a total of 224 proteins in sEVs and 680 proteins in m/lEVs identified across three patients (**Supplementary Table S5**). Glycopeptide searching retrieved a total of ~2300 glycoPSMs, covering 288 unique glycopeptides from 69 glycoproteins (**Supplementary Table S6**).

While under-glycosylation was a significant feature in sEVs and m/lEVs from HGSOC compared to non-cancerous cell lines, this finding was not observed in EVs from HGSOC and control ascites (Fig. 3**c**). Sialylation and fucosylation levels of sEVs from HGSOC and control ascites also

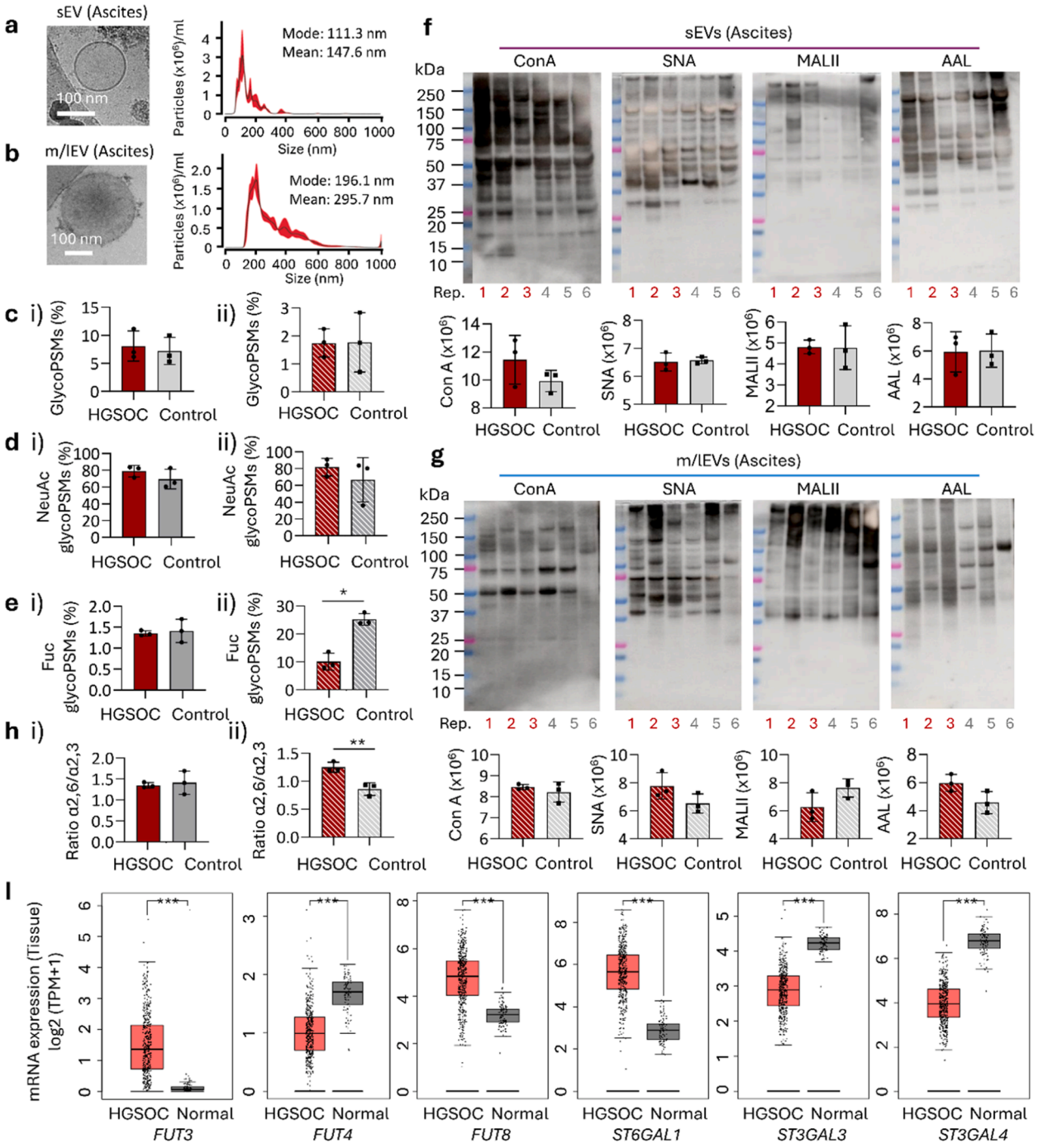

Fig. 3. Glycoprofile of EVs isolated from HGSOC and control ascites. Validation of sEVs (**a**) and m/lEVs (**b**) isolated from patient ascites using NTA and cryo-EM. Estimation of global (**c**) glycosylation, (**d**) sialylation, and (**e**) fucosylation levels relative to total glycoPSMs in sEVs (i) and m/lEVs (ii) isolated from HGSOC (n = 3) and control (n = 3) patient ascites. Lectin profiling of sEVs (**f**) and m/lEVs (**g**) using ConA, SNA, MALII and AAL lectins. (**h**) α2,6/α2,3-NeuAc ratio established by SNA/MALII lectin blotting in sEVs and m/lEVs from HGSOC and control patient ascites. (**i**) Gene expression profile of glycosylation enzymes in HGSOC tissues (n = 426) and non-cancerous tissues (n = 88). Significance set for $p < 0.001$ and log2 fold change (FC) > 1. Data obtained from TCGA and GTex database and accessed through GEPIA.

appeared similar as determined by glycopeptide analysis (Fig. 3**d-e**) and lectin blotting (Fig. 3**f**). The apparent discrepancy between the glycosylation efficiency of the investigated cell line-derived and the ascites-derived EVs can be attributed to the multiple cell sources contributing to the high complexity and heterogeneity of EVs found in patient ascites [32–34] unlike the homogenous cell line systems. The complex microenvironment found in patient tumor tissues is also an important factor shaping the glycosylation machinery and glycosylation profile of glycoproteins shed from tumor cells into body fluids [35,36], which is difficult to reproduce in cell line systems. Further studies are required to determine the cellular origins of the EVs in ascites to mechanistically explain the HGSOC-specific glycofeatures in ascites-derived EVs.

Glycopeptides carrying one fucose, which covered the majority of the fucosylated peptides, were significantly decreased in m/lEVs from HGSOC compared to control ascites (Fig. 3**e**), but this finding was not confirmed by AAL staining (Fig. 3**g**). The ambiguity in the determination of fucosyl linkage of glycans attached to glycoproteins in glycoproteomics and lectin blotting approaches is likely the reason for the disparate results from the two methods. AAL recognizes various fucosyl linkages (α1,2, α1,3, α1,4 and α1,6) attached to either an N-acetylglucosamine (GlcNAc) or N-acetyllactosamine related structures [37–39]. Except for α1,6-Fuc-GlcNAc, the other linkages can be found across various glycoconjugates including in N- and O-glycans and glycolipids [40,41]. In other words, AAL has reactivity towards different fucosyl linkages from various glycoconjugates. In contrast, glycoproteomics analysis was focused only on the identification of N-glycopeptides, where fine glycan structural information could not be confidently determined by the MS/MS assignments. Additional evaluation of the fine structural information of glycans [42], in particular the alterations in fucosylated glycans, is required to determine the clinical utility of this finding in HGSOC.

Notably, a significant increase of α2,6/α2,3-linked sialic acid ratio was observed using SNA/MALII lectin staining, which recapitulated the findings observed in cell lines (Fig. 3**g-h**). This result suggests that increased α2,6 sialylation in m/lEVs from ascites may represent a specific feature originating from HGSOC cells, holding a promising potential to be evaluated in larger cohort studies as a novel detection marker in HGSOC.

Aberrant sialylation and fucosylation have been widely reported as a hallmark in cancer contributing to tumor aggressiveness and immune evasion [43,44]. To explore the glycosylation machinery changes related to the aberrant sialylation and fucosylation observed in m/lEVs isolated from ascites of HGSOC patients, we investigated the mRNA expression of key fucosyltransferases and sialyltransferases in 426 HGSOC tissues and 88 normal tissues using public available transcriptomics data from TCGA and GTex. The expression of *FUT8* and *FUT3* were increased while the expression of *FUT4* was decreased in HGSOC compared to non-cancerous tissues (Fig. 3**i**). FUT8 drives the α1,6 core fucosylation while FUT3 and FUT4 are involved in the α1,3 antenna fucosylation. In OC, increased antenna fucosylation has been associated with the enhanced proliferation and invasiveness of cancer cells, contributing to tumor metastasis [45,46].

Remarkably, increase expression of the prominent α2,6-sialyltransferase *ST6GAL1*, and decrease expression of several α2,3-sialyltransferases *ST3GAL3* and *ST3GAL4* were observed in HGSOC tissues compared to non-cancerous tissues (Fig. 3**i**) and correlated with increased α2,6/α2,3-linked sialic acid ratio observed in HGSOC-derived m/lEVs from cell lines and patient ascites. In line with our findings, Wang et al, showed increase protein expression of ST6GAL1 and decrease protein expression of ST3GAL3 and 4 enzyme in OC compared to normal tissues [47]. Further, high mRNA expression of *ST6GAL1* in OC tissues was correlated with poor prognosis [48] and resistance to chemotherapeutic intervention [49]. Elevated sialylation was also reported in serum and ascites from OC patients [50–52] supporting the rationale for further investigation of this glycan feature in EVs from HGSOC patients in larger cohort of samples.

Collectively, these results have shown that aberrant sialylation in m/lEVs from ascites accompany HGSOC and pointed to some glycoenzymes in the glycosylation machinery that may be responsible for these changes in the OC tissues.

Conclusion

This study demonstrates that the N-glycoproteome of different populations of EVs can distinguish HGSOC from non-cancerous conditions. We observed key glycoproteome differences between sEVs and m/lEVs, which could serve as a reference dataset for further exploration of the glycobiology underlying EV function in HGSOC. Notably, α2,6-sialylation was found to be a prominent feature of HGSOC-derived m/lEVs from cell lines and ascites, which correlated with increase expression of *ST6GAL1* in HGSOC tissues. While further validation within a larger patient cohort is needed, the aberrant N-glycosylation of HGSOC-specific EVs presents opportunities for new diagnostic applications that could ultimately improve the treatment and survival of affected patients.

Funding sources

RK is supported by KAKENHI (24K17793 and 23K19347). MTA is supported by the Australian Research Council Future Fellowship (FT210100455). AY is supported by the Fusion Oriented Research for disruptive Science and Technology (FOREST; JPMJFR204J).

CRediT authorship contribution statement

Kristina Mae Bienes: Writing – original draft, Methodology, Formal analysis, Data curation. **Akira Yokoi:** Writing – original draft, Resources, Methodology, Funding acquisition, Data curation. **Masami Kitagawa:** Resources, Data curation. **Hiroaki Kajiyama:** Resources, Methodology. **Morten-Thaysen Andersen:** Writing – review & editing, Methodology, Data curation, Conceptualization. **Rebeca Kawahara:** Writing – original draft, Validation, Supervision, Project administration, Methodology, Investigation, Funding acquisition, Formal analysis, Data curation, Conceptualization.

Declaration of competing interest

The authors declare that they have no known competing financial interests or personal relationships that could have appeared to influence the work reported in this paper

Acknowledgments

We acknowledge the Division for Medical Research Engineering, Nagoya University Graduate School of Medicine and sincerely thank all patients who agreed to participate in the study.

Supplementary materials

Supplementary material associated with this article can be found, in the online version, at doi:10.1016/j.bbadva.2025.100140.

Data availability

The proteomics LC-MS/MS raw data and glycopeptide search results have been deposited to the ProteomeXchange Consortium via the PRIDE [16] partner repository with the dataset identifier: PXD056996.

References

[1] P.M. Webb, S.J. Jordan, Global epidemiology of epithelial ovarian cancer, Nat. Rev. Clin. Oncol. 21 (5) (2024) 389–400.

[2] J. Kim, E.Y. Park, O. Kim, J.M. Schilder, D.M. Coffey, C.H. Cho, R.C. Bast Jr., Cell origins of high-grade serous ovarian cancer, Cancers. (Basel) 10 (11) (2018) 433.
[3] L.C. Peres, K.L. Cushing-Haugen, M. Kobel, H.R. Harris, A. Berchuck, M.A. Rossing, J.M. Schildkraut, J.A. Doherty, Invasive epithelial ovarian cancer survival by histotype and disease stage, J. Natl. Cancer Inst. 111 (1) (2019) 60–68.
[4] A. Becker, B.K. Thakur, J.M. Weiss, H.S. Kim, H. Peinado, D. Lyden, Extracellular vesicles in cancer: cell-to-cell mediators of metastasis, Cancer Cell 30 (6) (2016) 836–848.
[5] L.A. McAlarnen, P. Gupta, R. Singh, S. Pradeep, P. Chaluvally-Raghavan, Extracellular vesicle contents as non-invasive biomarkers in ovarian malignancies, Mol. Ther. Oncolytics. 26 (2022) 347–359.
[6] J. Yu, S. Sane, J.E. Kim, S. Yun, H.J. Kim, K.B. Jo, J.P. Wright, N. Khoshdoozmasouleh, K. Lee, H.T. Oh, K. Thiel, A. Parvin, X. Williams, C. Hannon, H. Lee, D.K. Kim, Biogenesis and delivery of extracellular vesicles: harnessing the power of EVs for diagnostics and therapeutics, Front. Mol. Biosci. 10 (2023) 1330400.
[7] A. Yokoi, M. Ukai, T. Yasui, Y. Inokuma, K. Hyeon-Deuk, J. Matsuzaki, K. Yoshida, M. Kitagawa, K. Chattrairat, M. Iida, T. Shimada, Y. Manabe, I.Y. Chang, E. Asano-Inami, Y. Koya, A. Nawa, K. Nakamura, T. Kiyono, T. Kato, A. Hirakawa, Y. Yoshioka, T. Ochiya, T. Hasegawa, Y. Baba, Y. Yamamoto, H. Kajiyama, Identifying high-grade serous ovarian carcinoma-specific extracellular vesicles by polyketone-coated nanowires, Sci. Adv. 9 (27) (2023) eade6958.
[8] M.T. Briggs, M.R. Condina, M. Klingler-Hoffmann, G. Arentz, A.V. Everest-Dass, G. Kaur, M.K. Oehler, N.H. Packer, P. Hoffmann, Translating N-glycan analytical applications into clinical strategies for ovarian cancer, Proteom. Clin. Appl. 13 (3) (2019) e1800099.
[9] F.M. Wanyama, V. Blanchard, Glycomic-based biomarkers for ovarian cancer: advances and challenges, Diagnostics. (Basel) 11 (4) (2021) 643.
[10] R. Armbrister, L. Ochoa, K.L. Abbott, The clinical role of glycobiology on ovarian cancer progression, Adv. Cancer Res. 157 (2023) 1–22.
[11] J.A. Welsh, D.C.I. Goberdhan, L. O'Driscoll, E.I. Buzas, C. Blenkiron, B. Bussolati, H. Cai, D. Di Vizio, T.A.P. Driedonks, U. Erdbrugger, J.M. Falcon-Perez, Q.L. Fu, A. F. Hill, M. Lenassi, S.K. Lim, M.G. Mahoney, S. Mohanty, A. Moller, R. Nieuwland, T. Ochiya, S. Sahoo, A.C. Torrecilhas, L. Zheng, A. Zijlstra, S. Abuelreich, R. Bagabas, P. Bergese, E.M. Bridges, M. Brucale, D. Burger, R.P. Carney, E. Cocucci, R. Crescitelli, E. Hanser, A.L. Harris, N.J. Haughey, A. Hendrix, A. R. Ivanov, T. Jovanovic-Talisman, N.A. Kruh-Garcia, V. Ku'ulei-Lyn Faustino, D. Kyburz, C. Lasser, K.M. Lennon, J. Lotvall, A.L. Maddox, E.S. Martens-Uzunova, R.R. Mizenko, L.A. Newman, A. Ridolfi, E. Rohde, T. Rojalin, A. Rowland, A Saftics, U.S. Sandau, J.A. Saugstad, F. Shekari, S. Swift, D. Ter-Ovanesyan, J.P. Tosar, Z. Useckaite, F. Valle, Z. Varga, E. van der Pol, M.J.C. van Herwijnen, M.H. M. Wauben, A.M. Wehman, S. Williams, A. Zendrini, A.J. Zimmerman, M. Consortium, C. Thery, K.W. Witwer, Minimal information for studies of extracellular vesicles (MISEV2023): from basic to advanced approaches, J. ExtraCell Vesicles 13 (2) (2024) e12404.
[12] T.H. Chau, A. Chernykh, J. Ugonotti, B.L. Parker, R. Kawahara, M. Thaysen-Andersen, Glycomics-assisted glycoproteomics enables deep and unbiased N-glycoproteome profiling of complex biological specimens, Methods Mol. Biol. 2628 (2023) 235–263.
[13] Z. Tang, C. Li, B. Kang, G. Gao, C. Li, Z. Zhang, GEPIA: a web server for cancer and normal gene expression profiling and interactive analyses, Nucl. Acids Res. 45 (W1) (2017) W98–W102.
[14] W. Huang da, B.T. Sherman, R.A. Lempicki, Systematic and integrative analysis of large gene lists using DAVID bioinformatics resources, Nat. Protoc. 4 (1) (2009) 44–57.
[15] Z. Pang, L. Xu, C. Viau, Y. Lu, R. Salavati, N. Basu, J. Xia, MetaboAnalystR 4.0: a unified LC-MS workflow for global metabolomics, Nat. Commun. 15 (1) (2024) 3675.
[16] Y. Perez-Riverol, J. Bai, C. Bandla, D. Garcia-Seisdedos, S. Hewapathirana, S. Kamatchinathan, D.J. Kundu, A. Prakash, A. Frericks-Zipper, M. Eisenacher, M. Walzer, S. Wang, A. Brazma, J.A. Vizcaino, The PRIDE database resources in 2022: a hub for mass spectrometry-based proteomics evidences, Nucl. Acids Res. 50 (D1) (2022) D543–D552.
[17] A.C. Dixson, T.R. Dawson, D. Di Vizio, A.M. Weaver, Context-specific regulation of extracellular vesicle biogenesis and cargo selection, Nat. Rev. Mol. Cell Biol. 24 (7) (2023) 454–476.
[18] A. Beach, H.G. Zhang, M.Z. Ratajczak, S.S. Kakar, Exosomes: an overview of biogenesis, composition and role in ovarian cancer, J. Ovarian. Res. 7 (2014) 14.
[19] I. Khan, P.S. Steeg, Endocytosis: a pivotal pathway for regulating metastasis, Br. J. Cancer 124 (1) (2021) 66–75.
[20] A. Slomka, S.K. Urban, V. Lukacs-Kornek, E. Zekanowska, M. Kornek, Large extracellular vesicles: have we found the holy grail of inflammation? Front. Immunol. 9 (2018) 2723.
[21] N. de Haan, M. Song, O.C. Grant, Z. Ye, F. Khoder Agha, M. Koed Moller Aasted, R. J. Woods, S.Y. Vakhrushev, H.H. Wandall, Sensitive and specific global cell surface N-glycoproteomics shows profound differences between glycosylation sites and subcellular components, Anal. Chem. 95 (47) (2023) 17328–17336.
[22] H.C. Tjondro, I. Loke, S. Chatterjee, M. Thaysen-Andersen, Human protein paucimannosylation: cues from the eukaryotic kingdoms, Biol. Rev. Camb. Philos. Soc. 94 (6) (2019) 2068–2100.
[23] I. Loke, O. Ostergaard, N.H.H. Heegaard, N.H. Packer, M. Thaysen-Andersen, Paucimannose-rich N-glycosylation of spatiotemporally regulated human neutrophil elastase modulates its immune functions, Mol. Cell Proteom. 16 (8) (2017) 1507–1527.
[24] J. Ugonotti, R. Kawahara, I. Loke, Y. Zhu, S. Chatterjee, H.C. Tjondro, Z. Sumer-Bayraktar, S. Neelamegham, M. Thaysen-Andersen, N-acetyl-beta-D-hexosaminidases mediate the generation of paucimannosidic proteins via a putative noncanonical truncation pathway in human neutrophils, Glycobiology 32 (3) (2022) 218–229.
[25] W.W. Ren, R. Kawahara, K.G.N. Suzuki, P. Dipta, G. Yang, M. Thaysen-Andersen, M. Fujita, MYO18B promotes lysosomal exocytosis by facilitating focal adhesion maturation, J. Cell Biol. 224 (3) (2025).
[26] E. Machado, S. White-Gilbertson, D. van de Vlekkert, L. Janke, S. Moshiach, Y. Campos, D. Finkelstein, E. Gomero, R. Mosca, X. Qiu, C.L. Morton, I. Annunziata, A. d'Azzo, Regulated lysosomal exocytosis mediates cancer progression, Sci. Adv. 1 (11) (2015) e1500603.
[27] H. Lachuer, L. Le, S. Leveque-Fort, B. Goud, K. Schauer, Spatial organization of lysosomal exocytosis relies on membrane tension gradients, Proc. Natl. Acad. Sci. U.S.A. 120 (8) (2023) e2207425120.
[28] Y. Harada, Y. Ohkawa, Y. Kizuka, N. Taniguchi, Oligosaccharyltransferase: a gatekeeper of health and tumor progression, Int. J. Mol. Sci. 20 (23) (2019) 6074.
[29] Y. Hu, J. Pan, P. Shah, M. Ao, S.N. Thomas, Y. Liu, L. Chen, M. Schnaubelt, D. J. Clark, H. Rodriguez, E.S. Boja, T. Hiltke, C.R. Kinsinger, K.D. Rodland, Q.K. Li, J. Qian, Z. Zhang, D.W. Chan, H. Zhang, Clinical proteomic tumor analysis, integrated proteomic and glycoproteomic characterization of human high-grade serous ovarian carcinoma, Cell Rep. 33 (3) (2020) 108276.
[30] C. Williams, R. Pazos, F. Royo, E. Gonzalez, M. Roura-Ferrer, A. Martinez, J. Gamiz, N.C. Reichardt, J.M. Falcon-Perez, Assessing the role of surface glycans of extracellular vesicles on cellular uptake, Sci. Rep. 9 (1) (2019) 11920.
[31] C. Escrevente, S. Keller, P. Altevogt, J. Costa, Interaction and uptake of exosomes by ovarian cancer cells, BMC Cancer 11 (2011) 108.
[32] C.E. Ford, B. Werner, N.F. Hacker, K. Warton, The untapped potential of ascites in ovarian cancer research and treatment, Br. J. Cancer 123 (1) (2020) 9–16.
[33] S. Kim, B. Kim, Y.S. Song, Ascites modulates cancer cell behavior, contributing to tumor heterogeneity in ovarian cancer, Cancer Sci. 107 (9) (2016) 1173–1178.
[34] X. Zheng, X. Wang, X. Cheng, Z. Liu, Y. Yin, X. Li, Z. Huang, Z. Wang, W. Guo, F. Ginhoux, Z. Li, Z. Zhang, X. Wang, Single-cell analyses implicate ascites in remodeling the ecosystems of primary and metastatic tumors in ovarian cancer, Nat. Cancer 4 (8) (2023) 1138–1156.
[35] A. Fernandes, C.M. Azevedo, M.C. Silva, G. Faria, C.S. Dantas, M.M. Vicente, S. S. Pinho, Glycans as shapers of tumour microenvironment: a sweet driver of T-cell-mediated anti-tumour immune response, Immunology 168 (2) (2023) 217–232.
[36] E. Rodriguez, D.V. Lindijer, S.J. van Vliet, J.J. Garcia Vallejo, Y. van Kooyk, The transcriptional landscape of glycosylation-related genes in cancer, iScience 27 (3) (2024) 109037.
[37] J. Olausson, L. Tibell, B.H. Jonsson, P. Pahlsson, Detection of a high affinity binding site in recombinant Aleuria aurantia lectin, Glycoconj. J. 25 (8) (2008) 753–762.
[38] M. Fujihashi, D.H. Peapus, N. Kamiya, Y. Nagata, K. Miki, Crystal structure of fucose-specific lectin from Aleuria aurantia binding ligands at three of its five sugar recognition sites, Biochemistry 42 (38) (2003) 11093–11099.
[39] P.R. Romano, A. Mackay, M. Vong, J. DeSa, A. Lamontagne, M.A. Comunale, J. Hafner, T. Block, R. Lec, A. Mehta, Development of recombinant Aleuria aurantia lectins with altered binding specificities to fucosylated glycans, Biochem. Biophys. Res. Commun. 414 (1) (2011) 84–89.
[40] J. Hirabayashi, Development of lectin microarray, an advanced system for glycan profiling, Synthesiology 7 (2) (2014) 105–117.
[41] D. Wu, J. Li, W.B. Struwe, C.V. Robinson, Probing N-glycoprotein microheterogeneity by lectin affinity purification-mass spectrometry analysis, Chem. Sci. 10 (19) (2019) 5146–5155.
[42] A.V. Everest-Dass, J.L. Abrahams, D. Kolarich, N.H. Packer, M.P. Campbell, Structural feature ions for distinguishing N- and O-linked glycan isomers by LC-ESI-IT MS/MS, J. Am. Soc. Mass Spectrom. 24 (6) (2013) 895–906.
[43] A. Blanas, N.M. Sahasrabudhe, E. Rodriguez, Y. van Kooyk, S.J. van Vliet, Fucosylated antigens in cancer: an alliance toward tumor progression, metastasis, and resistance to chemotherapy, Front. Oncol. 8 (2018) 39.
[44] B.N. Vajaria, K.R. Patel, R. Begum, P.S. Patel, Sialylation: an avenue to target cancer cells, Pathol. Oncol. Res. 22 (3) (2016) 443–447.
[45] M. Tan, L. Zhu, H. Zhuang, Y. Hao, S. Gao, S. Liu, Q. Liu, D. Liu, J. Liu, B. Lin, Lewis Y antigen modified CD47 is an independent risk factor for poor prognosis and promotes early ovarian cancer metastasis, Am. J. Cancer Res. 5 (9) (2015) 2777–2787.
[46] J. Liu, B. Lin, Y. Hao, Y. Qi, L. Zhu, F. Li, D. Liu, J. Cong, S. Zhang, M. Iwamori, Lewis y antigen promotes the proliferation of ovarian carcinoma-derived RMG-I cells through the PI3K/Akt signaling pathway, J. Exp. Clin. Cancer Res. 28 (1) (2009) 154.
[47] P.H. Wang, W.L. Lee, C.M. Juang, Y.H. Yang, W.H. Lo, C.R. Lai, S.L. Hsieh, C. C. Yuan, Altered mRNA expressions of sialyltransferases in ovarian cancers, Gynecol. Oncol. 99 (3) (2005) 631–639.
[48] B. Wichert, K. Milde-Langosch, V. Galatenko, B. Schmalfeldt, L. Oliveira-Ferrer, Prognostic role of the sialyltransferase ST6GAL1 in ovarian cancer, Glycobiology 28 (11) (2018) 898–903.
[49] M.J. Schultz, A.T. Holdbrooks, A. Chakraborty, W.E. Grizzle, C.N. Landen, D. J. Buchsbaum, M.G. Conner, R.C. Arend, K.J. Yoon, C.A. Klug, D.C. Bullard, R. A. Kesterson, P.G. Oliver, A.K. O'Connor, B.K. Yoder, S.L. Bellis, The tumor-associated glycosyltransferase ST6Gal-I regulates stem cell transcription factors and confers a cancer stem cell phenotype, Cancer Res. 76 (13) (2016) 3978–3988.

[50] S. Miyamoto, L.R. Ruhaak, C. Stroble, M.R. Salemi, B. Phinney, C.B. Lebrilla, G. S. Leiserowitz, Glycoproteomic analysis of malignant ovarian cancer ascites fluid identifies unusual glycopeptides, J. Proteome Res. 15 (9) (2016) 3358–3376.
[51] K. Biskup, E.I. Braicu, J. Sehouli, R. Tauber, V. Blanchard, The ascites N-glycome of epithelial ovarian cancer patients, J. Proteom. 157 (2017) 33–39.
[52] A.Y. Berghuis, J.F.A. Pijnenborg, T.J. Boltje, J.M.A. Pijnenborg, Sialic acids in gynecological cancer development and progression: Impact on diagnosis and treatment, Int. J. Cancer 150 (4) (2022) 678–687.